

Table II. Frequency and Fluence Dependence of per Pulse Yields and Stationary States

alkene	$\nu_{\text{ex}}, \text{cm}^{-1}$	$10^{19} \sigma_t, \text{cm}^2$	$10^{19} \sigma_c, \text{cm}^2$	fluence, J/cm ²	$10^5(\text{yield/pulse})^b$		steady state, ^c % cis
					t \rightarrow c	c \rightarrow t	
2-butene	975	1.4	0.5	4.5	30	<0.1	(<95)
2-pentene	949	0.17	0.15	4.5	1.0	0.13	88
				6.0	7.0	0.69	91
crotononitrile	931	0.64	0.09	3.2	70	<0.1	99 (>95)
				5.5	90	1	98 (>95)
				3.4	80	<0.1	99 (>95)
1,3-pentadiene	931	2.7	2.4	2.7	310	210	60 (63)
				2.7	41	12	77 (80)
				2.9	145	44	77 (80)
				3.1	310	89	78 (80)
				2.7	300	<0.1	(<95)
	982	3.2	2.1	2.7	300	<0.1	(<95)

^a Single-photon absorption cross section obtained from infrared absorption spectrum ($\pm 10\%$). ^b Yield of molecules in irradiated volume converted per pulse at low conversions (<5%). ^c Values calculated from single-pulse yields or the observed stationary state (values in parentheses).

($\pm 20\%$) with the single-photon absorption cross sections. Additionally, plots of the average number of photons absorbed per pulse vs. laser fluence are linear over the fluence range 1–3.5 J/cm². Such behavior is characteristic of large organic molecules for which excitation from the region of discrete states to the quasi-continuum occurs without the threshold behavior observed for small molecules.^{2,3,13}

The most striking result of the present investigation is that essentially quantitative (>95%) contrathermodynamic conversion of trans to cis alkenes can be achieved in cases where the ratio of single-photon absorption cross section $\sigma_t/\sigma_c > 1.5$. Even in those cases where the difference in cross section is small ($\sigma_t/\sigma_c = 1.1 \pm 0.1$ for 2-pentene and for 1,3-pentadiene at 931 and 953 cm⁻¹), the percent cis isomer content of the stationary state is significantly higher than predicted from the ratio of cross sections. Thus substantial amplification of the difference in single-photon absorption cross section may occur in the multiphoton excitation process. The results for 1,3-pentadiene demonstrate that even with the limited selection of excitation frequency available with the CO₂ TEA laser, it is possible to control the isomer ratio by the choice of frequency.

The per pulse yields for trans \rightarrow cis isomerization (Table II) are dependent upon alkene structure, absorption cross section, and laser fluence. Both *trans*-2-butene and *trans*-2-pentene display a threshold fluence of ca. 4 J/cm², below which the per pulse yield is too small to permit accurate measurement (<10⁻⁶). Threshold fluences for *trans*-crotononitrile and *trans*- or *cis*-1,3-pentadiene are 1.5 J/cm². Above these threshold values, yields increase with increasing laser fluence, as shown in Table II for 953-cm⁻¹ irradiation of 1,3-pentadiene and 1049-cm⁻¹ irradiation of 2-pentene. Irradiation of *trans*-2-butene with fluence >6 J/cm² induces more fragmentation than isomerization, while irradiation of *cis*- or *trans*-1,3-pentadiene at 982 cm⁻¹ and at fluences >3 J/cm² results in loss of H₂ to quantitatively and irreversibly yield cyclopentadiene.¹⁴ This in itself is an interesting result. It is another example^{2b} where merely changing laser parameters can drastically alter the course of a reaction. Comparison of the results for *trans*-2-butene and *trans*-2-pentene demonstrates that the yield increases with increasing absorption cross section for molecules with similar activation barriers irradiated with the same laser fluence. While differences in cross section and fluence preclude quantitative comparison of results for the different alkenes, it is clear that the per pulse yield also increases with decreasing thermal activation energy (Table I). These observations are consistent with a simple rate equations model for reversible multiphoton isomerization in which the yield is determined by the convolution

of state populations (determined by absorption cross section and laser fluence) and isomerization rate constants.^{3b}

Acknowledgment. Support of this work by the National Science Foundation through Grants CHE79-08501 to E.W. and CHE80-26020 to F.D.L. is gratefully acknowledged. The CO₂ TEA laser was purchased under NSF Grant CHE76-84494A01.

Registry No. *cis*-2-Butene, 590-18-1; *cis*-crotononitrile, 1190-76-7; *cis*-1,3-pentadiene, 1574-41-0; *trans*-2-butene, 624-64-6; *trans*-crotononitrile, 627-26-9; *trans*-1,3-pentadiene, 2004-70-8; *cis*-2-pentene, 627-20-3; *trans*-2-pentene, 646-04-8.

²⁵²Cf Fission Fragment Ionization Mass Spectrometry of Chlorophyll *a*

B. T. Chait* and F. H. Field

Rockefeller University, New York, New York 10021

Received May 24, 1982

In a recent communication, Hunt et al.¹ report on the fission fragment induced ionization mass spectra of chlorophyll *a* (Chl *a*). They conclude that the fragmentation reactions observed must have occurred on an extremely short time scale (10⁻¹²–10⁻¹⁴ s). We have made an independent investigation of Chl *a* by fission fragment ionization mass spectrometry. We obtain new results, and our conclusions differ substantially from those of the aforementioned authors.¹

The mass spectra were obtained with the spectrometer described previously,² modified³ by the addition of retarding grids to allow the measurement of reactions and rates of decompositions occurring during flight. A flux of 3000 fission fragments s⁻¹ was used. Samples with a thickness of $\sim 15 \mu\text{g}/\text{cm}^2$ were prepared by evaporation of Chl *a* from benzene and CCl₄ solutions on 1 μm thick Ni and 2 μm thick aluminized polyester, respectively.

Our unretarded spectra of Chl *a* correspond closely to those given in ref 1. The molecular ion regions of the sharpened spectra obtained with retarding potential are shown in Figure 1, top (positive), and Figure 1, bottom (negative). The Chl *a* sample contained a small amount of pheophytin *a* (Pheo *a*), which serves a useful comparative function.

The following observations were made:

(1) Only 1.3% of the positive and 4.7% of the negative Chl *a* molecular ions survive intact the 67- μs flight to the ion detector.

(13) Nguyen, H. H.; Danen, W. C. *J. Am. Chem. Soc.* **1981**, *103*, 6253–6255.

(14) (a) Loss of H₂ in the low-pressure pyrolysis of 1,3-pentadiene is reported to yield 1,2,4-pentatriene on the basis of a *m/e* 66 peak in the mass spectrum.^{14b} We found that the IR spectrum, mass spectral fragmentation, and GC retention time of the *m/e* 66 product were identical with those of cyclopentadiene. (b) Nguyen, T. T.; King, K. D. *Int. J. Chem. Kinet.* **1982**, *14*, 623–629.

(1) Hunt, J. E.; Macfarlane, R. D.; Katz, J. J.; Dougherty, R. C. *J. Am. Chem. Soc.* **1981**, *103*, 6775–6778.

(2) Chait, B. T.; Agosta, W. C.; Field, F. H. *Int. J. Mass Spec. Ion Phys.* **1981**, *39*, 339–366.

(3) Chait, B. T.; Field, F. H. *Int. J. Mass. Spec. Ion Phys.* **1981**, *41*, 17–29.

(4) Samples of Chl *a* were obtained from the Laboratory of D. C. Mauzerall at The Rockefeller University, The Sigma Chemical Co., St. Louis, MO, and United States Biochemical Corp., Cleveland, OH.

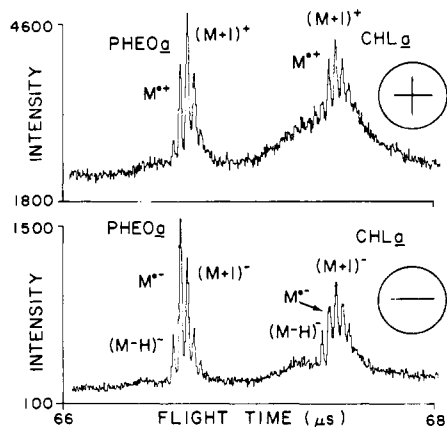


Figure 1. Positive (top) negative (bottom) molecular ion regions.

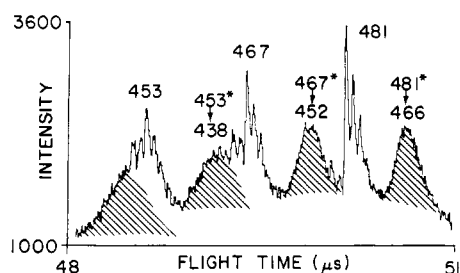


Figure 2. Portion of fragment region of positive spectrum with applied retarding potential. The shaded peaks are flight tube fragment ions. Their position in the spectrum is displaced by the retarding potential.

The corresponding figures for Pheo *a* are 13% and 26%, respectively, indicating a significantly lower decomposition probability for Pheo *a* compared to Chl *a*.

(2) The Chl *a* peak labeled⁵ $(M + 1)^+$ in Figure 1, top, contains a substantial component of $(M + H)^+$ ion.³ Similarly, both M^+ and $(M + H)^+$ molecular ions are observed for the Pheo *a* portion of the spectra of Figure 1, top.

(3) The most intense ion in the Chl *a* molecular ion region of the negative spectrum (Figure 1, bottom) is $(M + 1)^-$, which corresponds formally to the addition of H^- to neutral chlorophyll.⁶ By contrast, the $(M + 1)^-$ intensity in the Pheo *a* molecular ion region is completely accounted for by the ¹³C contribution from the adjacent M^- ion. Thus we have the interesting observation that the centrally coordinated Mg atom in chlorophyll appears to be necessary for the formation of this entity.

(4) $(M - H)^-$ ions appear in both the Chl *a* and Pheo *a* portions of the negative spectra.

The presence of $(M + H)^-$ and $(M - H)^-$ in the spectra of Chl *a* has not previously been reported.⁷ Hunt and co-workers,^{1,8} using a lower resolution apparatus, report only the presence of M^+ and M^- ions in the molecular weight region of Chl *a*.

Fragmentations that take place in the flight tube occur with rate constants in the range 10^4 – 10^7 s⁻¹. Spectra were taken with (1) no retarding potential and (2) with a retarding potential large enough to reject ions produced by fragmentations in the flight tube. 71% of the positive ions with $m/z > 350$ entering the flight tube fragment in it. The corresponding value for negative ions is 40%.

By the application of carefully controlled retarding potentials, the identities of the various fragmentation reactions occurring in

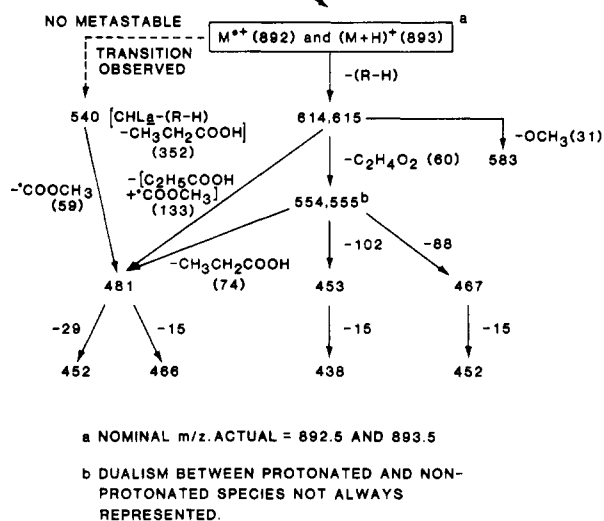
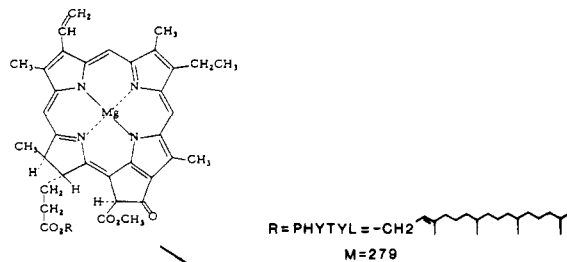


Figure 3. Map of positive ion flight tube fragmentations.

the flight tube can be established.^{3,9} For example, the shaded peaks in Figure 2 correspond to flight tube fragment ions. The separation of the center of the fragment peak from the corresponding sharp reactant peak establishes the mass of the neutral fragment loss. The neutral fragment losses shown in Figure 1 are 15 ± 1 . This technique was used to elucidate the majority of the strong flight tube fragmentations for positive ions (Figure 3).

More specific information about fragmentation rate constants was obtained from experiments made with a short low-field portion (0.6 cm) in the ion acceleration region. Fragmentations occurring in the low-field portion can be specifically detected and rate constants deduced. For example, the rate constant for the reaction $M^+ \rightarrow 614^+ + 278$ was determined to be $(4.4 \pm 0.4) \times 10^6$ s⁻¹ for reaction occurring 0.23×10^{-6} s after the ion producing event.

Mass peaks in the spectra may exhibit asymmetries toward high times resulting from fragmentations in the acceleration region.³ Information about the rate constants of the fragmentations can be deduced from the shapes of these high-time tails and the applied accelerating field. For example, the m/z 614 peak exhibits a tail from which one can deduce the occurrence of $M^+ \rightarrow 614^+ + 278$ with rate constants ranging from 10^6 to 10^7 s⁻¹. The summed intensities of the ions with $10^8 > k > 10^7$ s⁻¹ are comparable to that of the sharp m/z 614 peak ($k > 10^8$ s⁻¹).

Retarding potential measurements have been made on negative ions from Chl *a*, and a network of flight tube fragmentations has been deduced completely analogous to that depicted in Figure 3. In summary, flight tube fragmentations occur from and to all of the strong negative ions in the spectrum with $m/z > 350$ (40% of all ions fragment). Most important, a flight tube fragmentation of the molecular ions (M^- , $(M + 1)^-$) to m/z 613, 614 occurs with strong intensity, which demonstrates unequivocally that negative molecular ions with large intensity enter the flight tube and then decompose.

A main hypothesis of Hunt et al.¹ is that because of energetic reasons, fragmentation in Chl *a* occurs "explosively", that is, in

(5) Careful calibration of the mass scale with the $Cs(CsI)_2^+$ and $Cs(CsI)_3^+$ ions allowed the determination of the molecular ion peak masses with a standard deviation of 30 mnu.

(6) Hydride ion addition to molecules has been observed: DePuy, C. H.; Bierbaum, V. M.; Schmitt, R. J.; Shapiro, R. H. *J. Am. Chem. Soc.* **1978**, *100*, 2920–2921.

(7) All of these results were well reproduced with three Chl *a* samples obtained from different sources.⁴

(8) Hunt, J. E.; Macfarlane, R. D.; Katz, J. J.; Dougherty, R. C. *Proc. Natl. Acad. Sci. U.S.A.* **1980**, *77*, 1745–1748.

(9) Hunt, W. W.; Huffman, R. E.; McGee, K. E. *Rev. Sci. Instr.* **1964**, *35*, 82–87.

times in the range 10^{-14} – 10^{-12} s ($k = 10^{12}$ – 10^{14} s $^{-1}$). Our results demonstrate (1) much fragmentation occurs with rate constants in the range 10^4 – 10^8 s $^{-1}$; (2) roughly equal amounts of fragmentation with rate constants greater and less than 10^8 s $^{-1}$ occurs; (3) a wide range of rate constants exists for each fragmentation; (4) a relatively slow fragmentation of the negative molecular ions occurs.

We can make no direct measurement of reaction rates larger than 10^8 s $^{-1}$. Reactions with such rates obviously occur (prompt reactions).

Our findings lead us to suggest that the fission fragment induced fragmentation processes involve many of the concepts embodied in the quasi-equilibrium theory of mass spectra, e.g., the formation of reactant ions with a wide range of energies, which results in a network of sequential and competing unimolecular reactions with variable and wide-ranging rate constants. This is contrary to the hypothesis of Hunt and co-workers.

Acknowledgment. This work was supported in part by the Division of Research Resources, National Institutes of Health.

Registry No. Chlorophyll a, 479-61-8.

Aldol Methodology: Synthesis of Versatile Intermediates. 3-Hydroxy-2-vinylcarbonyl Compounds

Satoru Masamune,*† Tatsuo Kaiho, and David S. Garvey

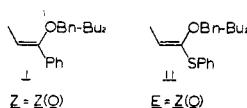
Department of Chemistry
Massachusetts Institute of Technology
Cambridge, Massachusetts 02139

Received May 20, 1982

Reaction of an aldehyde with the chiral *Z*(*O*)-enolate **1** or **1a**,¹ followed by simple modification of the resulting aldol product, constitutes an enantioselective synthesis of a *syn*-3-hydroxy-2-methylcarboxylic acid (**2** or **2a**) (Scheme I),^{2,3} a fundamental

[†]The work outlined in this and the following communications was presented by S.M. at the 24th Bachmann Memorial lecture at the University of Michigan on April 15 and 16, 1982, and also was outlined in September 1981 at several German universities, including the University of Cologne.

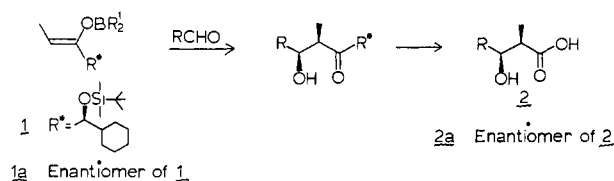
(1) The two boron enolates **i** and **ii** shown below are designated *Z* and *E*. Since very often we are concerned with the relative disposition of the OBn-Bu₂ and methyl groups with respect to the double bond, it is preferred to assign the same descriptor to **i** and **ii**. We propose the use of *Z*(*O*), indicating that top priority is conferred on the element in the bracket in this special case.



(2) (a) Masamune, S.; Choy, W.; Kerdesky, F. A. J.; Imperiali, B. *J. Am. Chem. Soc.* **1981**, *103*, 1566. (b) Masamune, S.; Ali, Sk. A.; Snitman, D. L.; Garvey, D. S. *Angew. Chem., Int. Ed. Engl.* **1980**, *19*, 557. Also see: (c) Evans, D. A.; Bartroli, J.; Shih, T. L. *J. Am. Chem. Soc.* **1981**, *103*, 2127.

(3) Assignment of the *R* or *S* configuration to each chiral center unambiguously defines the relative stereochemistry of any pair of the chiral centers existing in a molecule. However, as erythro and threo used in conjunction with the Fischer projection formula have served to express conveniently the stereochemical relationship between the substituents attached to the adjacent carbon atoms of a saccharide molecule, it is expedient to have stereochemical descriptors associated with the zigzag formula that is now commonly used for the acyclic system. The use of "syn" and "anti" previously proposed^{2b} to describe two (non-hydrogen) substituents on the same side and those on the opposite side of the plane defined by the zigzag main chain has the advantage of *instant recognition* of relative configuration. If there are more than two (non-hydrogen) substituents attached to a pair of carbon atoms, the substituent of the highest priority at each carbon atom is chosen to designate the relative stereochemistry. Thus, "syn" and "anti" is perhaps the simplest of any stereochemical description designed for the acyclic system where the main chain is clearly identified. This is indeed very often the case. These descriptors may be replaced by any of other pairs of words, "con and dis", "like and unlike", "same and opposite", etc., with the exception of erythro and threo. The recent usage of these latter words in aldol chemistry is confusing and conflicts with the convention adopted in carbohydrate chemistry. These two areas of chemistry are now closely related. Recently, S.M. has received preprints from Professors D. Seebach and V. Prelog and also from Professor F. A. Carey, both proposing new sets of descriptors through the extension of the Cahn-Ingold-Prelog system. We gratefully appreciate the information.

Scheme I



structural unit embedded in numerous natural products of propionate origin.⁴ It has been demonstrated that such aldol reactions indeed play the major role in constructing the carbon framework of the complex metabolite 6-deoxyerythronolide B, which contains ten chiral centers.⁵ While this achievement represents a major breakthrough in the development of the aldol methodology, further generalization of this approach demands solutions to several other problems. Two of them are the enantioselective synthesis of (1) *anti*-3-hydroxy-2-methyl carbonyl compounds (**3**) (for this introductory paragraph see the compounds in boxes in Scheme II) and, more importantly, (2) systems represented by compounds **4** and **5**, which correspond to the C(13)–C(19) fragment of amphotericin B (**6**)⁶ and the C(11)–C(17) fragment of tylonolide (for the structure see the following two communications⁷), respectively. Note that both **4** and a synthetic precursor⁸ of **5** carry two hydroxyl groups at the β and β' positions to a carbonyl group. These two problems now find a simultaneous solution: All of the compounds **3**–**5** are derived from the common intermediate **7** or **7a** (see the bold arrows in Scheme II), a compound accessible via a diastereoselective aldol reaction using the new chiral reagent **8** or **8a**. We outline herein the strategy for the construction of these unique structural units and then describe in the following communication⁷ the synthesis of tylonolide, the aglycone of the 16-membered polyoxomacrolide antibiotic tylosin.⁴

Synthesis of Reagents 8 and 8a (Scheme III). Treatment of *R*-hexahydromandelic acid (**9**)^{2a} with 3.5 equiv of cyclopropyl-lithium⁹ in ether provides the cyclopropylketone **10**, which is in turn converted to its *tert*-butyldimethylsilyl derivative (**11**) (83% overall yield). Heating a benzene solution of **11** with 1 equiv of lithium benzeneselenolate in the presence of 12-crown-4 at 70 °C¹⁰ opens the cyclopropane ring to yield the 3-benzeneseleno ketone **8** (91%). The use of *S*-hexahydromandelic acid (**9a**)² in this sequence leads naturally to the preparation of the enantiomer (**8a**) of **8**, and thus both the *S* and *R* isomers of the reagent are available.

Preparation of 7 and 7a (Scheme III). Generation of the dicyclopentylboron enolate from **8** and subsequent aldol condensation with 3.5 equiv of propanal is performed in the standard fashion^{2,11} to provide the expected 2,3-syn product **12** in 97% yield (based on **8**) and with >100:1 diastereoselection. The high yield and selectivity observed in this reaction with **8** are general for a variety of achiral aldehydes (e.g., **7a**). After desilylation, elimination of the benzeneselenol group from **12** [ozonization at –78 °C followed by warming (50 °C) the resulting selenoxide in hexane containing pyridine¹²] proceeds well and affords **13** in 86% overall

(4) For a review of the chemistry and biochemistry of macrolide antibiotics, see: Masamune, S.; Bates, G. S.; Corcoran, J. W. *Angew. Chem., Int. Ed. Engl.* **1977**, *16*, 585.

(5) Masamune, S.; Hiram, M.; Mori, S.; Ali, Sk. A.; Garvey, D. S. *J. Am. Chem. Soc.* **1981**, *103*, 1568.

(6) Ganis, P.; Avitabile, G.; Mechlini, W.; Schaffner, C. P. *J. Am. Chem. Soc.* **1971**, *93*, 4560. Mechlini, W.; Schaffner, C. P.; Ganis, P.; Avitabile, G. *Tetrahedron Lett.* **1970**, 3873.

(7) Masamune, S.; Lu, L. D.-L.; Jackson, W. P.; Kaiho, T.; Toyoda, T. *J. Am. Chem. Soc.*, following communication in this issue.

(8) Such as compound **22**: see Scheme II.

(9) Seyferth, D.; Cohen, H. M. *J. Organomet. Chem.* **1963**, *1*, 15.

(10) Smith, A. B., III; Scarborough, R. M., Jr. *Tetrahedron Lett.* **1978**, 1649.

(11) Propanal, which is inexpensive, was used in excess. A 1:1 mixture of an aldehyde and the boron enolate normally leads to an approximately 80% yield of the aldol product.

(12) (a) Reich, H. J.; Renga, J. N.; Reich, I. L. *J. Am. Chem. Soc.* **1975**, *97*, 5434. (b) Reich, H. J.; Wollowitz, S.; Trend, J. E.; Chow, F.; Wendelborn, D. F. *J. Org. Chem.* **1978**, *43*, 1697.